ELSEVIER

Contents lists available at www.sciencedirect.com

## Journal of the European Ceramic Society

journal homepage: www.elsevier.com/locate/jeurceramsoc



# Effect of HfO<sub>2</sub> addition as intergranular grains on the energy storage behavior of Ca<sub>0.6</sub>Sr<sub>0.4</sub>TiO<sub>3</sub> ceramics



Lin Zhang, Hua Hao, Hanxing Liu\*, Zhe Song, Zhonghua Yao, Juan Xie, Haixia Liu, Xinyi Zhu, Qi Xu, Xuechen Huang, Minghe Cao

State Key Laboratory of Advanced Technology for Materials Synthesis and Processing, School of Material Science and Engineering, Wuhan University of Technology, Wuhan 430070, China

#### ARTICLE INFO

Article history: Received 12 January 2016 Received in revised form 26 April 2016 Accepted 2 May 2016 Available online 12 May 2016

Keywords: Linear CST Intergranular grains Breakdown strength Energy storage efficiency Interfacial polarization

#### ABSTRACT

Pore free  $Ca_{0.6}Sr_{0.4}TiO_3$  (CST) ceramics with  $HfO_2$  additives (0 wt.%, 2.0 wt.%, 4.0 wt.% and 6.0 wt.%) were fabricated via solid state reaction method at  $1400\,^{\circ}C$ . Structure characterization was conducted by XRD and SEM, indicating the existence of  $HfO_2$  at grain boundaries as the intergranular phase. The dielectric breakdown strength and energy storage efficiency were found to be greatly enhanced for CST with moderate  $HfO_2$  additives, the sample with 4.0 wt.%  $HfO_2$  exhibited optimized microstructure and energy storage properties, with maximum average breakdown strength (28.9 kV/mm) and high energy storage efficiency (nearly 95% at  $24\,\text{kV/mm}$ ). In addition, effect of Hf-rich intergranular phase on the charge transportation and interfacial polarization behavior was discussed. With good dispersion, the intergranular  $HfO_2$  phase was considered effective to modify the grain boundaries properties and consequently improve the energy storage performance for CST ceramics.

© 2016 Elsevier Ltd. All rights reserved.

#### 1. Introduction

The high intrinsic dielectric breakdown strength (BDS), low dielectric loss and favorable temperature and bias voltage stability enable  $\text{Ca}_{1-x}\text{Sr}_x\text{TiO}_3$  (x=0-1) (CST) ceramics potential in the electric energy storage applications. However, lower BDS in practice and the drop of energy storage efficiency under high electric field inhibits their commercial prospects. Interfacial polarization was believed to contribute to the BDS and energy storage efficiency in polycrystalline ceramics as an effective extrinsic factor [1-7], except for porosity [8], grain size [9,10] and secondary phase [11]. Thus, enhanced macroscopic performance of CST system can be achieved by tailoring interfacial polarization behavior.

Extensive efforts have been devoted to the modification of interfacial polarization in glass ceramics, among them, the research work of Ming-Jen Pan was impressive for the discovery that the modification of glass phase with higher resistivity was more effective than that of ceramic phase [12], which provided some inspiration that the modification of grain boundary is decisive in ceramic materials for its resistive nature. Various approaches for the grain boundary modification were proposed [9,13–15], includ-

ing intergranular phases introduction. Liebault found that fine  $\rm ZrO_2$  intergranular phase with good dispersion in  $\rm Al_2O_3$  ceramics is beneficial to modify the nature of the grain boundary, accounting for progressively diffused charges and effectively improved breakdown strength [15]. So it is interesting to reference this method for interfacial polarization tailoring and discuss the relationship between the modified microstructure and the improved electric properties.

In the present work, we chose  $Ca_{0.6}Sr_{0.4}TiO_3$  as the matrix, considering the optimized microstructure and energy storage behavior for CST composition with x=0.4 crossover the phase transition region. HfO<sub>2</sub>, known as promising high- $\kappa$  insulator [16] with wide band gap of 5.6 eV [17], was selected for intergranular phase at grain boundaries. Compared to the matrix (band gap  $\approx$ 3–4 eV [18]), Hfrich intergranular grains exhibit higher insulating nature, beneficial for charge transportation between grains and grain boundaries, which may lead to the suppression of interfacial polarization. In addition, three quantitative methods of interfacial polarization were employed to verify its effect on degraded energy storage performance.

Corresponding author.

E-mail address: lhxhp@whut.edu.cn (H. Liu).

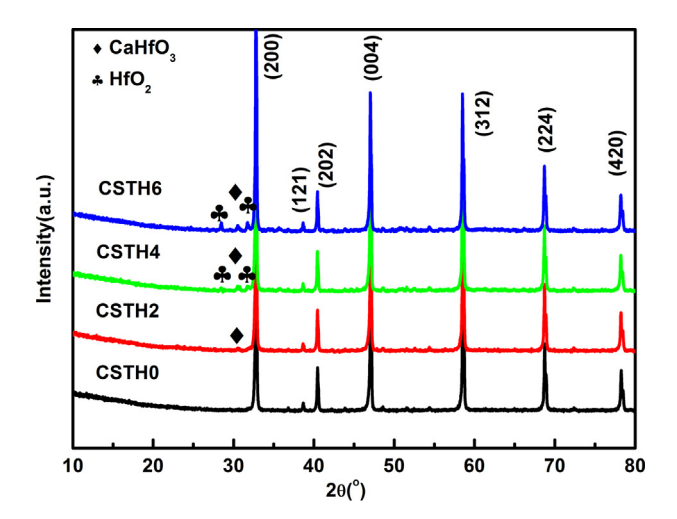


Fig. 1. XRD patterns of CSTH ceramics.

#### 2. Experimental procedure

#### 2.1. Samples preparation

Ca $_{0.6}$ Sr $_{0.4}$ TiO $_3$  ceramics with HfO $_2$  additives (0 wt.%, 2.0 wt.%, 4.0 wt.% and 6.0 wt.%) (simplified as CSTH0, CSTH2, CSTH4, CSTH6, respectively) were fabricated via solid state reaction method. CaCO $_3$ , SrCO $_3$ , TiO $_2$  and HfO $_2$  powders with high purity were used as raw materials. CaCO $_3$ , SrCO $_3$  and TiO $_2$  powders were mixed and ball milled with zirconium media in ethanol for 24 h. After dried, the powders were calcined in air at 1200 °C for 2 h and mixed with stoichiometrical HfO $_2$  additives (0 wt.%, 2.0 wt.%, 4.0 wt% and 6.0 wt.%) for ball milling. Discs with 12 mm in diameter and 1 mm in thickness were uniaxially pressed under a pressure of 200 MPa and sintered at 1400 °C for 2 h.

#### 2.2. Structural characterization

XRD analysis was performed on the as-sintered and polished pellets using Cu K\alpha radiation (X'Pert PRO, PANalytical, Holland). Microstructure was observed on thermally etched crosssection of the sintered samples by field-emission scanning electron microscope (HR-SEM) (Quanta FEG 450, FEI, USA). Impedance spectroscopy was measured using a precision impedance analyzer (E4980A, Agilent, USA) connected with an external furnace. To determine the polarization versus electric field (P-E) hysteresis loops, the sintered samples were polished to 0.3 mm in thickness and measured by ferroelectric material test system (HVI0403-239, Radiant Technology, USA) in a silicone oil bath, using triangular voltage waveforms at a frequency of 10 Hz. The charged/discharged energy storage density was estimated from the P-E curves, by integrating the area enclosed within the polarization axis and the charged/discharged curve. The energy storage efficiency was decided by the ratio of discharged and charged energy density.

#### 3. Results and discussion

#### 3.1. Structure analysis

Fig. 1 shows the XRD patterns of all samples sintered at 1400 °C. Two different secondary phases can be observed with increasing  $HfO_2$ , being confirmed to be  $CaHfO_3$  (00-008-0236) and  $HfO_2$  (01-078-0049), located at  $2\theta = 31^\circ$  and  $27^\circ$ ,  $33^\circ$ , respectively, according to the JCPDS card. The concentration of secondary phases was observed to increase with higher  $HfO_2$  contents.

**Table 1** The calculated values of a, b and c (Å) lattice parameters.

	а	b	С
CSTH0	5.463	5.452	7.726
CSTH2	5.465	5.451	7.729
CSTH4	5.465	5.450	7.729
CSTH6	5.461	5.454	7.731

The uncertainties in a, b and c were in the range of  $\pm 0.0005$  to  $\pm 0.001$ .

**Table 2**Relative permittivity and dielectric loss of CSTH ceramics at room temperature and temperature stability of capacitance.

	$\varepsilon_{\rm r}$	tanδ	$T_{\text{max}}(\Delta C/C_{\text{RT}} \leq \pm 15\%)  (^{\circ}\text{C})$
CSTH0	243 (±3)	6‰ (±0.2‰)	97 (±1)
CSTH2	$242 (\pm 2)$	6‰ (±0.3‰)	94 (±1)
CSTH4	$240 (\pm 2)$	$7\% (\pm 0.1\%)$	96 (±2)
CSTH6	$244(\pm 3)$	$5\% (\pm 0.4\%)$	95 (±2)

Fig. 2(a) exhibits enlarged XRD peaks around  $2\theta$  =  $33^{\circ}$ , where no obvious peak shift was found, indicating that HfO<sub>2</sub> may not incorporate into the lattice because of larger ionic radius of Hf<sup>4+</sup> (0.079 nm) than Ti<sup>4+</sup> (0.069 nm). For further analysis, Si standard sample was added into CSTH ceramic powders to eliminate systematic error. As seen in Fig. 2(b–d), Si (111), (220) and (311) peaks were used to calibrate (200), (004) and (312) peaks of CSTH, and calculate lattice parameters a, c and b respectively, using the formula  $1/d^2 = h^2/a^2 + k^2/b^2 + l^2 + c^2$ . The calculated a, b and c were found to slightly changed with the variation of HfO<sub>2</sub> (seen in Table 1), revealed the exclusive distribution of HfO<sub>2</sub> at grain boundaries.

Fig. 3 gives the cross-section SEM images of CSTH ceramic samples thermal etched at 1350 °C for 30 min, the dense microstructures were obtained. Greatly reduced grain size together with detectable intergranular grains was observed with the addition of HfO<sub>2</sub>. Additionally, in Fig. 4 which gives backscattered SEM images of CSTH ceramics, heterogenous distribution of intergranular grains and non-uniform grain size was revealed for CSTH6, due to excess addition of HfO<sub>2</sub>. Thus, structure analysis by XRD and SEM indicates that Hf-rich intergranular phase at grain boundaries were introduced successfully, consistent with our research expectation.

#### 3.2. Energy storage behaviors

The dielectric properties of CST ceramics with Hf-rich intergranular phase over the temperature range of 25 °C to 150 °C was analyzed and listed in Table 2. The intrinsic relative permittivity of HfO<sub>2</sub> was reported to be 18 [19], which is much smaller than CST (240). However, the addition of HfO<sub>2</sub> has limited effect on the dielectric properties of CST, probably due to its small concentration and special existence type as intergranular grains.

Fig. 5 shows the Weibull distribution of the breakdown strength for CSTH ceramics, which was believed most appropriate for the BDS analysis, described by [20,21]:

$$X_i = ln(E_i) \tag{1}$$

$$Y_i = \ln(-\ln(1 - P_i))$$
 (2)

$$P_i = \frac{i}{1+n} \tag{3}$$

where  $X_i$  and  $Y_i$  are two parameters in Weibull distribution function,  $E_i$  is the specific breakdown field of each specimen,  $P_i$  is the probability for dielectric breakdown, n is the sum of specimens of each sample, and i is the serial number of specimen. The samples were arranged in ascending order of BDS values as:

$$E_1 \leq E_2 \leq \ldots \leq E_i \leq \ldots \leq E_n(4)$$

### Download English Version:

# https://daneshyari.com/en/article/1473655

Download Persian Version:

https://daneshyari.com/article/1473655

<u>Daneshyari.com</u>